

RSC Advances



This is an *Accepted Manuscript*, which has been through the Royal Society of Chemistry peer review process and has been accepted for publication.

Accepted Manuscripts are published online shortly after acceptance, before technical editing, formatting and proof reading. Using this free service, authors can make their results available to the community, in citable form, before we publish the edited article. This *Accepted Manuscript* will be replaced by the edited, formatted and paginated article as soon as this is available.

You can find more information about *Accepted Manuscripts* in the [Information for Authors](#).

Please note that technical editing may introduce minor changes to the text and/or graphics, which may alter content. The journal's standard [Terms & Conditions](#) and the [Ethical guidelines](#) still apply. In no event shall the Royal Society of Chemistry be held responsible for any errors or omissions in this *Accepted Manuscript* or any consequences arising from the use of any information it contains.

Cite this: DOI: 10.1039/c0xx00000x

www.rsc.org/xxxxxx

PAPER

Electron scattering from germanium tetrafluoride

Biplab Goswami, Rahla Naghma and Bobby Antony*

Received (in XXX, XXX) Xth XXXXXXXXX 20XX, Accepted Xth XXXXXXXXX 20XX

DOI: 10.1039/b000000x

This paper describes the use of two methodologies to find electron impact total cross sections (TCS) from 1-5000 eV. The *ab initio* R-matrix method is used at low impact energies and the spherical complex optical potential (SCOP) formalism at intermediate to high energies. The TCS from both formalisms match quite well at the overlapping energy (~12 eV) allowing us to predict cross section for such a wide energy range. Besides TCS, calculations for electronic excitation, rotational excitation, momentum transfer and differential elastic cross sections are also reported using the R-matrix method. At low incident energies the presence of a broad resonant feature at 5.69 eV due to degenerate 2B_1 , 2B_2 and 2B_3 states is observed, revealing the probability of anion formation by electron attachment process and further decay to neutral and negative ion fragments. The electronic and rotational excitation cross sections for e-GeF₄ scattering are reported for the first time.

I. Introduction

Germanium tetrafluoride (GeF₄) is an important commonly used industrial inorganic fluoride. It has attracted much attention to fibre optics industry for its applications in ion implantation processes owing to the high refractive index and low optical dispersion of GeO₂¹. This molecule has also importance in the semiconductor manufacturing processes, particularly as a guest molecule to decrease the germanium-related bond density in thin films for plasma-enhanced chemical vapour deposition (CVD) processes². The Ge semiconductor films play crucial role in low-pressure chemical vapour deposition (LPCVD) because of the feasibility of depositing a uniform large-area film³. GeF₄ is the main source of fluorine for low-temperature thin film growth in thermal chemical deposition⁴. Hence, gas phase studies on e-GeF₄ scattering, which involves many important processes such as ionization, excitation and dissociation, become imperative.

In spite of various technological applications there have been only limited studies on electron collisions with GeF₄ molecule. The lone measurement of electron impact total cross section (TCS) was conducted by Szmytkowski *et al.*⁵ using a linear transmission experimental setup for impact energies from 0.5 to 250 eV. Kato *et al.*⁶ measured elastic cross sections by electron impact in the energy range 3-200 eV applying crossed electron molecular beam spectrometers. Calculations on 3-200 eV electron impact total cross sections of GeF₄ were reported by Kato *et al.*⁶ using independent atom model - screen corrected additivity rule (IAM-SCAR) method. The calculated elastic cross section for e-GeF₄ was also reported using an independent atom model (IAM) by Mozejko *et al.*⁷ from 50 to 2000 eV.

The remaining part of the paper is presented in three sections. The “Theoretical Methodology” gives a brief description of the salient features of the methods adopted for the present calculation. The “Results and Discussion” describes the results of the present study. Finally, “Conclusion” depicts the inferences derived from the results obtained in this work.

II. Theoretical Methodology

Two distinct methodologies are used in the present calculations. The low energy computations were carried out using the *ab initio* R-matrix method⁸ through Quantemol-N package⁹. The spherical complex optical potential (SCOP)¹⁰⁻¹³ formalism is employed for the high energy calculations. The *ab initio* R-matrix method is suitable for low energies typically below the ionization threshold of the target, whereas SCOP formalism provides satisfactory results for energies above the ionization threshold to 5 keV. All the calculations were performed within a fixed nuclei approximation at the equilibrium configuration of the molecule. We will first discuss the target model before going into the details of theoretical methodology employed in the low energy calculations.

A. Target model.

The accuracy of scattering cross sections data obtained by the R-matrix method primarily depends on the accurate representation of the target wave functions. GeF₄ is a tetrahedral molecule with a bond length of 1.68 Å¹⁴. For the present calculations a 6-311G Gaussian basis set is used for the target wave function representation, since it yields reasonable target parameters for the

GeF₄ molecule. For low energy calculations the target is represented by D₂ point group instead of T_d due to the restriction of the R-matrix code. The ground-state Hartree-Fock electronic configuration for the GeF₄ molecule is represented as 1a², 2a², 1b₂², 1b₁², 1b₃², 2b₂², 2b₁², 2b₃², 3a², 4a², 3b₂², 3b₁², 3b₃², 4b₂², 4b₁², 4b₃², 5a², 6a², 7a², 5b₃², 5b₁², 5b₂², 8a², 6b₂², 6b₁², 6b₃², 9a², 10a², 7b₁², 7b₂², 7b₃², 8b₃², 8b₁², 8b₂². Out of the 68 electrons, 56 core electrons were frozen, while the remaining 12 electrons were allowed to move freely in active space. A total number of 3951 configuration state functions (CSFs) are used in close coupling expansion to represent thirteen target states. The number of channels included in the R-matrix calculations is 79. We have used large number of CSFs to ensure a better determination of resonance positions at low-energies. The target parameters were generated by constructing the transition density matrix utilizing GAUSPROP and DENPROP¹⁵ modules of the UK R-matrix software suite. The multipole transition moments in the inner region were calculated using the second-order perturbation theory and the property integrals computed by GAUSPROP.

The present calculation produces a ground state energy of -2473.26 Hartree for the GeF₄ molecule, which is in good accord with the theoretical value of -2473.24 Hartree¹⁶. The present rotational constant of 0.116 cm⁻¹ matches very well with the theoretical value of 0.116 cm⁻¹¹⁶. The computed dipole moment for GeF₄ is zero which agrees with the previously measured dipole moment⁶. The first electronic excitation energy for GeF₄ is found to be 11.97 eV. The target properties along with the available comparisons are listed in Table 1.

Table 1 Target properties.

Properties of GeF ₄	Present	Others
Ground-state energy (hartree)	-2473.26	-2473.24 ¹⁶
First excitation energy (eV)	11.97	-
Rotational constant (cm ⁻¹)	0.116	0.116 ¹⁶
Dipole moment (D)	0	0 ⁶

B. Low energy formalism (1 eV ~ 18 eV)

There are various theoretical methods viz. the Kohn variational method¹⁷, the Schwinger multichannel method¹⁸ and the *ab initio* R-matrix method to treat low energy electron molecule scattering problem. However, the R-matrix formalism is the most widely used approach. The basic idea behind the R-matrix method is the division of configuration space into two distinct regions namely an inner region and an outer region. The inner region is taken as a sphere centred at the centre of mass of the target molecule. The inner region (R-matrix) radius is chosen such that it encompasses the entire electronic charge density (or wave functions) of the target states employed in the calculation. The scattering electron and the target electrons become indistinguishable creating a complex numerical problem in the inner region. The interaction

potential dominating in this region comprises of static, exchange and correlation polarisation potentials, which are short range in nature. However, in the outer region, the exchange and correlations are assumed to be negligible and only the long-range multipolar interactions between the scattering electron and the target are included. A single-centre close coupling approximation is undertaken in the outer region which produces quick solutions. Here, the spatial distribution is an outcome of electronic charge distribution around the centre of mass of the system. For the present system the inner R-matrix radius is taken as 13 a.u., while the outer region calculations are extended up to 100 a.u.

For the construction of the wave function in the inner region, the close-coupling (CC) approximation¹⁹ is used. Then it is applied to solve the time independent Schrödinger equation. The inner region wave function can be expressed as,

$$\psi_k^{N+1} = A \sum_l \psi_l^N(x_1, \dots, x_N) \sum_j \zeta_j(x_{N+1}) a_{ljk} + \sum_m \chi_m(x_1, \dots, x_{N+1}) b_{mk} \quad (1)$$

where A is the anti-symmetrization operator. ζ_j is a continuum orbital spin coupled with the scattering electron, x_N is the spatial and spin coordinate of the N^{th} electron, and a_{ljk} and b_{mk} are variational coefficients. The target plus continuum states are used in the close-coupled expansion. The static exchange calculation has a single Hartree-Fock target state in the first summation. The second summation runs over configurations χ_m , where all the electrons are located in the target molecular orbitals. The close-coupled calculation includes the lowest number of target states, represented by a configuration interaction (CI) expansion in the first term and over a 100 configurations in the second, including the orthogonality relaxation and short-range polarisation effects.

The occupied and virtual molecular target orbitals are constructed using the Hartree-Fock Self-Consistent Field method with Gaussian-type orbitals and the continuum orbitals of Faure *et al.*²⁰ In the present calculation we have included up to g orbital ($l = 4$). The R-matrix acts as a bridge between the inner region and outer region. The R-matrix computed at the boundary of the inner region is propagated to large scattering distance, where the radial equation describing the scattering electron is matched with the analytical expressions given by Gailitis expansion²¹. This matching gives K -matrices, which are diagonalised to obtain the eigenphase sum. The eigenphase sum is further used to calculate the position and width of the resonances using the resonance detection program RESON²² by matching it to Breit-Wigner profile²³. The K -matrices are also used to determine T -matrices by the definition,

$$T = \frac{2iK}{1-iK} \quad (2)$$

These T matrices are in turn used to obtain various cross sections¹⁹. The differential cross sections (DCS) and rotational cross sections are calculated using the POLYDCS program of Sanna and Gianturco²⁴.

C. High energy formalism.

The SCOP method is employed to find the cross sections in the intermediate to high energy region. The electron-molecule interaction dynamics is represented by a complex potential of the form,

$$V_{opt}(r, E_i) = [V_{st}(r) + V_{ex}(r, E_i) + V_p(r, E_i)] + i[V_{abs}(r, E_i)] \quad (3)$$

Here E_i represents the energy of the incident electron. V_{st} is the static potential, obtained from the parameterised Hartree-Fock wave functions of Cox and Bonham²⁵ and V_{ex} is the local exchange potential, determined from the parameter free Hara's free electron gas exchange potential²⁶. V_p is the polarisation potential which accounts for the long range interaction and short range correlation effect, formulated from the parameter free model of correlation polarisation potential given by Zhang *et al*²⁷. The absorption potential, V_{abs} stands for the total loss of scattered flux into all the allowed channels of electronic excitation and ionization. This is represented by the non-empirical quasi-free model of Staszewska *et al*²⁸. This absorption potential can be expressed as,

$$V_{abs}(r, E_i) = -\rho(r) \sqrt{\frac{T_{loc}}{2}} \left(\frac{8\pi}{10k_f^3 E_i} \right) \theta(p^2 - k_f^2 - 2\Delta) \times (A_1 + A_2 + A_3) \quad (4)$$

where the parameters A_1 , A_2 and A_3 are defined as,

$$A_1 = \frac{5k_f^3}{2\Delta}; \quad (5a)$$

$$A_2 = -\frac{k_f^3(5p^2 - 3k_f^3)}{(p^2 - k_f^2)^2} \quad (5b)$$

$$\text{and } A_3 = 2\theta(2k_f^2 + 2\Delta - p^2) \frac{(2k_f^2 + 2\Delta - p^2)^{5/2}}{(p^2 - k_f^2)^2} \quad (5c)$$

The local kinetic energy of the incident electron is given by,

$$T_{loc} = E_i - (V_{st} + V_{ex} + V_p) \quad (6)$$

In Eqn. (4) $p = \sqrt{2E_i}$ and $k_f = [3\pi^2 \rho(r)]^{1/3}$ are the momentum and Fermi wave vectors respectively. $\rho(r)$ is the radial charge density of the target calculated by the single centre expansion method using parameterised Hartree-Fock wave functions of Cox and Bonham²³. In this method the target is assumed to be spherical and hence the charge density and static potential is obtained through a single centre expansion technique. This approximation is justified here as the target molecule is tetrahedral and closely packed. Further, $\theta(x)$ is the Heaviside unit step-function and Δ is an energy dependent parameter below which $V_{abs} = 0$. Here $\Delta = I$, where I is the ionization threshold of the target, as considered in the original model of Staszewska²⁶. The non spherical terms arising due to molecular vibration and rotation can be neglected in the full expansion of the absorption potential, as they are not significant at the present energy range.

After generating the full complex optical potential given in Eqn.

(3), the radial Schrödinger equation for e-GeF₄ scattering is solved using the method of partial wave analysis. The complex phase shifts (δ_l) for each partial wave are obtained as the solution of the scattering equation, which are further used to calculate the inelasticity or absorption factor given by,

$$\eta_l = \exp(-2 \text{Im } \delta_l) \quad (7)$$

Using this inelasticity factor the relevant cross sections viz., Q_{el} and Q_{inel} can be obtained²⁹ through the following expressions:

$$Q_{el}(E_i) = \frac{\pi}{k^2} \sum_{l=0}^{\infty} (2l+1) |\eta_l \exp(\text{Re } \delta_l) - 1|^2 \quad (8)$$

and

$$Q_{inel}(E_i) = \frac{\pi}{k^2} \sum_{l=0}^{\infty} (2l+1) (1 - \eta_l^2) \quad (9)$$

By adding these two cross sections we get the total cross section. The SCOP formalism adopted here is an established method for calculating total cross section, typically in the intermediate to high electron impact energies.

III. Results and Discussions

In this section the results obtained employing the present computational methods are depicted. The total cross sections obtained by two distinct formalisms are found to match smoothly at the overlapping energy (~12 eV), allowing us to predict the cross sections over a wide energy range from 1 eV to 5 keV. Figs. 1-6 and Table 3, presents the results obtained from this study.

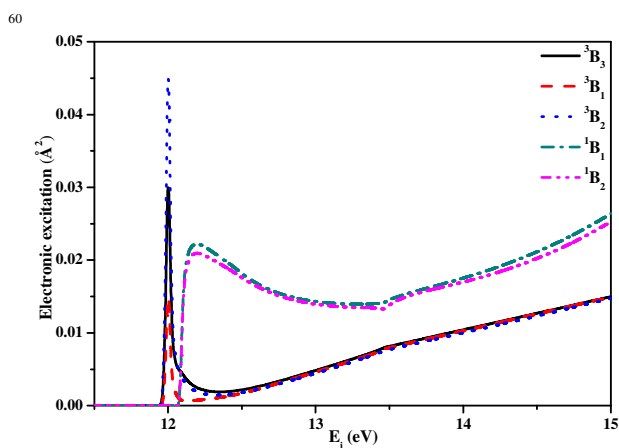


Fig. 1. Electronic excitation cross section for e-GeF₄ scattering.

Fig.1 displays the electronic excitation cross section for e-GeF₄ scattering. ³B₃, ³B₁ and ³B₂ electronic states exhibit excitation threshold at 11.97 eV, whereas ¹B₁ and ¹B₂ states show a threshold of 12.08 eV. The sharp peaks obtained for the electron excitation cross sections at about 12 eV are due to ³B₂, ³B₁ and ³B₂ states. Another maximum is visible at 12.2 eV due to ¹B₁ and ¹B₂ states. The sharp peaks observed in Fig. 1 may be because of the core-excited shape resonances. These resonances arise due to the trapping of electron temporarily in the empty valence orbitals.

No previous electronic excitation cross sections data is available in the literature for this molecule to compare our results.

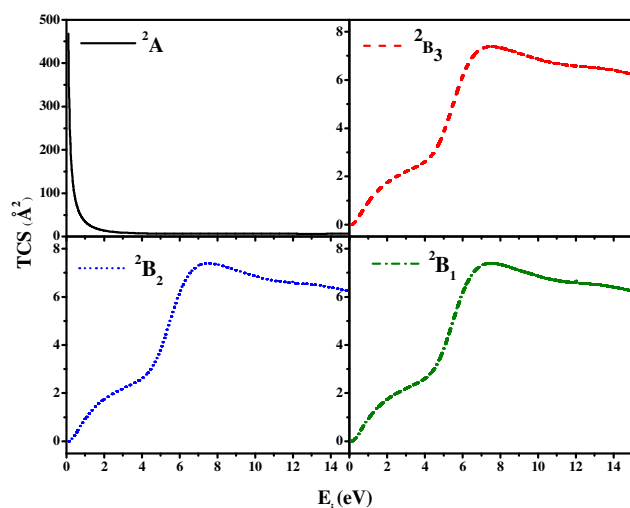


Fig. 2. Symmetry component of the elastic cross section for electron scattering by GeF_4 .

The elastic cross sections for different symmetry component of e- GeF_4 scattering are plotted in Fig. 2. Here we can see that, at very low energies the maximum contribution of elastic cross sections comes from the 2A symmetry of the D_2 point group, whereas the other three symmetries (2B_1 , 2B_2 and 2B_3) show similar structure and contributing maximum at about 5-7 eV. From Fig. 2, we can observe that these three symmetries (2B_1 , 2B_2 and 2B_3) show shape resonances at 5.69 eV belonging to the T_1 symmetry of the T_d group, which splits into the 2B_1 , 2B_2 , and 2B_3 symmetries of the D_2 point group. Table 2, gives the correlation of the symmetry between the T_d and D_2 point groups. Bjarnason *et al.*³⁰ reported the energy of dissociation for the formation of GeF_3^- , GeF_2^- , GeF^- and F^- anions from GeF_4 molecule. The present calculation predicts a resonance at 5.69 eV, which is in fair agreement with the dissociation energy of 5 eV, as measured by Bjarnason *et al.*²⁸ for the formation of F^- from GeF_4 . Since the resonance width predicted here is 3.55 eV, it is assumed that the hump in the TCS curve (Fig. 3) around 7.36 eV is due to the contributions from T_1 symmetry of T_d .

Table 2. Correlation table between T_d and D_2 point groups.

T_d group	D_2 group	Resonances (eV)	
		Position	Width
A_1	A	-	-
A_2	A	-	-
E	$2A$	-	-
T_1	$B_1+B_2+B_3$	5.69	3.55
T_2	$B_1+B_2+B_3$	5.69	3.55

30

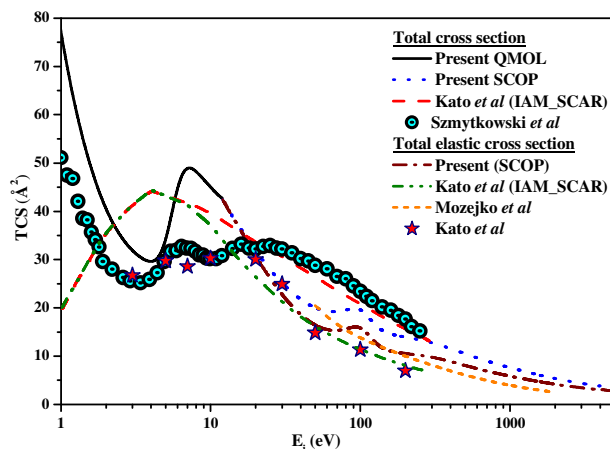


Fig. 3. Total cross section for e- GeF_4 scattering in Å^2 . Solid line: Present, QMOL (Q_T), dotted line: Present SCOP (Q_T), circles-dots: Szmytkowski *et al.*⁵ (Q_T), dashed dotted line: Present SCOP (Q_{el}), dashed line: Kato *et al.* (IAM_SCAR) (Q_{el})⁶, short dashed line: Mozejko *et al.* (Q_{el})⁷, stars: Kato *et al.* (Q_{el})⁶.

The electron impact total cross section for the GeF_4 molecule is displayed in Fig. 3 and the respective cross section values are tabulated in Table 3. At the low energy region the present TCS is the sum of elastic, electronic excitation and rotational excitation cross sections. At very low energies below 5 eV, present result shows qualitative agreement with the only experimental study⁵. The present peak at around 7.36 eV and the minima at about 3.64 eV are in good agreement with that of the experimental values reported by Szmytkowski *et al.*⁵ and the elastic cross sections of Kato *et al.*⁶. The appearance energies and peak intensity position of ion yield for various negative fragments of GeF_4 upon electron impact were reported to be from 5-7 eV and 7-8 eV respectively²⁸. The broad resonance identified at 5.69 eV with width 3.55 eV in the present study falls in the 5-7 eV range. At energies above 50 eV, present result agrees very well with the measurements of Szmytkowski *et al.*⁵ and with the IAM_SCAR calculations Kato *et al.*⁶. Independent atom model cannot satisfactorily predict cross section at low incident energies and can be employed safely for energies greater than 20 eV⁶. This aspect is clearly depicted from Fig. 3, where we can see that the characteristic shown by IAM_SCAR is entirely different compared to present results as well as of Szmytkowski *et al.*⁵. However, towards the high energy region, IAM_SCAR show reasonable agreement with other data. IAM_SCAR breaks down below 20 eV due to the fact that it cannot deal with the case of an electron temporarily binding to the target, as happens for the present scattering system. After 300 eV, there are no previous data available for the total cross sections to compare our results. The present elastic cross section gives satisfactory agreement with that of Mozejko *et al.*⁷ and Kato *et al.*⁶. In general present total and elastic cross sections show qualitative and quantitative agreement with previous results.

70

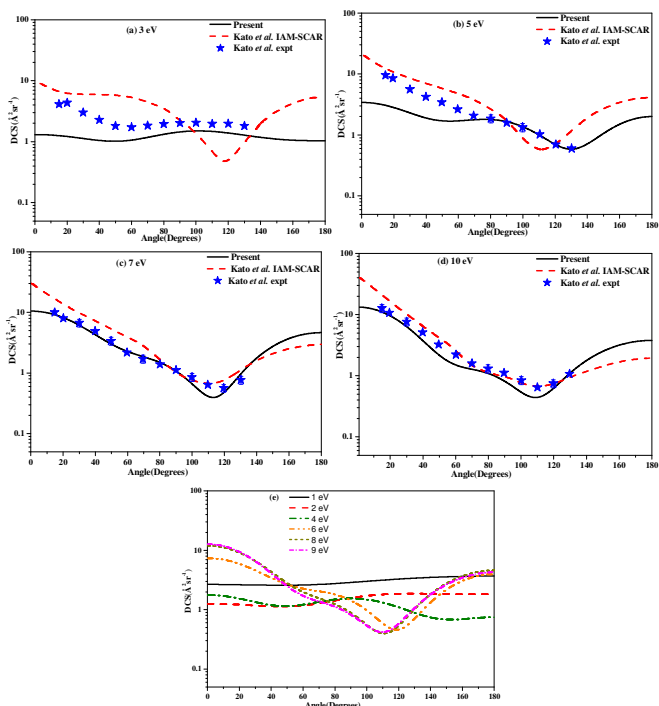


Fig. 4. DCSs for e-GeF₄ scattering at different energies. In figures 4(a-d), solid line: Present, dashed line: Kato *et al.* (IAM_SCAR)⁶, stars: Kato *et al.* expt.⁶

5

The electron impact differential elastic cross sections (DCS) obtained for the e-GeF₄ scattering are plotted in Fig. 4. Determination of DCS is the stringent test for any scattering theory, as it is sensitive to the effects which are averaged over in the case of integral cross section. Previous results are available for 3, 5, 7 and 10 eV. The angular distribution of 3 eV DCS is entirely different than those at energies greater than 5 eV. Although the present DCS at 3 eV is significantly lower than the experimental values⁶ at forward angles, it shows qualitative agreement with experiment⁶. At 5 eV, present results are quite lower than the experimental DCS of Kato *et al.*⁶ at forward scattering angles. However, beyond 60 degrees they match quite nicely as shown in fig.4 (b). This discrepancy at low energies and scattering angles less than 60° can be ascribed to the difficulty in representing the polarisability of the target, since the low angle behavior depends mainly on long range interaction. At impact energies beyond 5 eV, we observe strong forward peaking in the DCS curve in accordance with the experimental findings⁶. This can be attributed to the high dipole polarisability of the GeF₄ molecule (6.5 Å³), which plays an important role in direct scattering processes and diminishes progressively at low impact energies. From Figs. 4 (c) and (d), we can see that present DCS at 7 eV and 10 eV shows excellent agreement with the experiment of Kato *et al.*⁶ in terms of magnitude and shape. From Fig. 4, it is noticeable that the position of DCS minima is shifted backward for higher impact energies. Overall the comparison of present data with that of Kato *et al.*⁶ is quite reasonable at various angles. In Fig. 4 (e) we have plotted all other DCS data together for energies from 1 eV to 9 eV where comparisons are not available. From this figure we can get an overall idea about the angular

35

distribution of elastic cross section in terms of shape and magnitude.

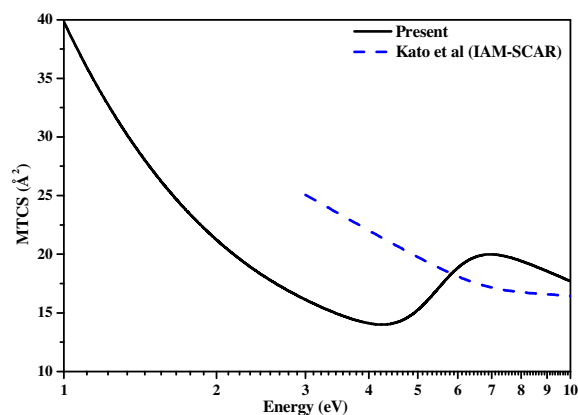


FIG. 5. Momentum transfer cross sections for e-GeF₄ scattering system. Solid line: Present, dashed line: Kato *et al.* (IAM_SCAR)⁶.

Fig. 5 represents the momentum transfer cross sections (MTCS) by electron impact with GeF₄ molecule at low impact energies along with the only available data of Kato *et al.*⁶ MTCS data are used as input in the simulation code for kinetic transport modellers to study the behaviour of electrons as they drift and diffuse, under the influence of an applied electric field or crossed electric and magnetic fields through the gas. Hence, these cross sections are very important to such studies. In figure 5 we can see that at very low energies, typically below 6 eV, the present result become quite low and shows a dip at around 4-5 eV. Also, present MTCS data depicts a clear hump at about 7 eV. Both these features are clearly missing in the calculation of Kato *et al.*⁶. Kato *et al.*⁶ have reported theoretical MTCS derived from the DCSs using the IAM_SCAR computations. The disagreement between the present result and the IAM_SCAR result of Kato *et al.*⁶ for the compared energy range is quite similar to that of the DCSs curve presented in Fig. 4. Large variation between the present and previous results is observed for energies below 7 eV. This overestimation of cross section may be due to the inaccurate representation of the target wave function by independent atom model. However, as the impact energy increases the deviation becomes quite low. Furthermore the comparison (disagreement) between the present values and IAM_SCAR⁶ results are quite consistent for both TCS and MTCS for the compared energy region.

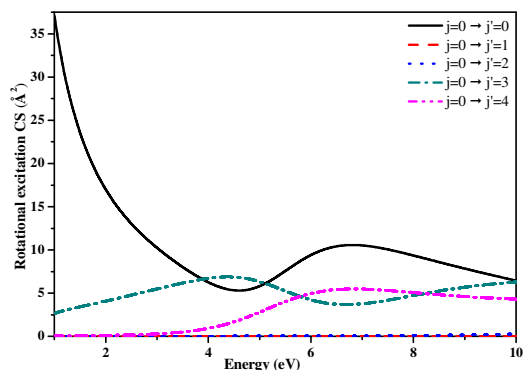


FIG. 6. Rotational excitation cross sections for e-GeF₄ scattering.

The electron impact rotational excitation cross sections for $j=0 \rightarrow j'=0, 1, 2, 3, 4$ states of GeF₄ molecule is plotted in Fig. 6. The maximum contribution of cross section comes from the $j=0 \rightarrow j'=0$ state. For low energies the rotational elastic cross section by $j=0 \rightarrow j'=0$ state becomes considerably high. When the speed of the incident electron is less at low energies, electron gets enough time to impart a rotational force on the molecule. From Fig. 6, it is quite clear that the rotational excitation cross section for the $j=0 \rightarrow j'=1$ and $j=0 \rightarrow j'=2$ becomes negligible, since there is no dipole or quadruple moment acting for the present target. However, the rotational excitation cross section for the $j=0 \rightarrow j'=3$ and $j=0 \rightarrow j'=4$ are significant. The broad structure in rotational excitation cross section at around 7 eV, particularly for $j=0 \rightarrow j'=0$ and $j=0 \rightarrow j'=4$ states, also coincides with the hump in total cross sections as displayed in Fig. 3.

Table 3 TCS for e-GeF₄ scattering.

Energy (eV)	TCS (Å ²) (QMOL)	Energy (eV)	TCS (Å ²) (SCOP)
1.0	77.22	12	42.55
1.5	51.67	14	40.79
2.0	40.53	16	38.73
2.5	34.94	18	36.97
3.0	31.91	20	35.49
3.5	30.22	30	30.68
4.0	29.62	40	28.61
4.5	30.67	50	27.21
5.0	34.18	100	20.10
5.5	39.59	150	16.91
6.0	44.64	200	15.07
6.2	46.13	250	13.67
6.4	47.28	300	12.58
6.6	48.09	350	11.71
6.8	48.61	400	11.98
7.0	48.89	450	10.37
7.2	48.97	500	9.88
7.4	48.91	600	9.06
7.6	48.75	700	8.40
7.8	48.51	800	7.84
8.0	48.22	900	7.37
8.2	47.90	1000	6.96
8.4	47.57	1100	6.59
8.6	47.24	1200	6.29

8.8	46.90	1300	6.01
9.0	46.57	1400	5.75
9.5	45.76	1500	5.53
10.0	45.01	2000	4.66
10.5	44.30	3000	3.63
11.0	43.66	4000	3.03
11.5	43.09	5000	2.63

IV. Conclusion

An extensive theoretical work has been performed to evaluate electron impact cross sections for GeF₄ molecule. The primary aim of this work is to investigate all the major electron impact scattering phenomena occurring over an extensive energy range from 1 eV to 5000 eV. This is the first ever report on electron driven collision processes on such an energy scale. It is a well known fact that low energy electrons (< 10eV) can induce short lived anions (resonances), which may subsequently decay to produce neutral and anionic fragments. The local chemistry of any environment where such processes takes place, primarily intermediate to high energy electron scattering cross sections are important in the study of technological plasma, semiconductor manufacturing industry, atmospheric physics, astrophysics and radiation physics. Hence, it is quite obvious that electron impact scattering cross sections over a wide energy range from meV to keV is imperative in the study of chemical processes in various fields. Thus, the aim of work reported is twofold: (1) to present the electron impact total cross sections over an extensive energy range (1-5000 eV) and (2) to detect the position of resonances if any, at low energies. We have detected a resonance at 5.69 eV with a width of 3.55 eV. The broad width is typical to a shape resonance. This is found to be due to the ²B₁, ²B₂ and ²B₃ symmetries (T₁ symmetry), which is reproduced as a pronounced hump in the TCS curve. We have also presented total elastic cross sections for different scattering symmetries. The present TCS results depict reasonable agreement with the experiment of Szymtkowski *et al*⁵. The present DCSs also show qualitative agreement with the measurement of Kato *et al*⁶. We have also compared our data with the theoretical values reported by the same group using IAM_SCAR method. The DCS and MTCS also show consistent comparison with available data. The electronic and rotational excitation cross sections presented here are reported for the first time.

As discussed earlier, various cross sections for GeF₄ upon electron impact are pertinent to the fields like plasma etching, semiconductor manufacturing and microelectronics. However, cross section data for various scattering channels covering a wider energy domain were lacking. This has motivated us to take up this work. The R-matrix method is an accurate *ab initio* method suitable particularly at low impact energies, below 15 eV. Its accuracy relies on the basis set used for the construction of wavefunctions, which is confirmed by the accuracy with which it produces the target parameters. The uncertainty in the R-matrix

calculation cannot be obtained rigorously. However, the calculations can be repeated in several ways: (1) employing different basis sets, (2) changing R-matrix radius, (3) increasing the size of CAS, (4) increasing the number of states included and then the sensitivity to these changes may be estimated. In the present calculation we have optimised the above parameters to a limit before computation fails, without compromising the results. The SCOP method is primarily a high energy formalism, employed above the ionization threshold of the target to 5000 eV. Both methods are found to give consistent results in their respective energy regime for the molecule of present study. The results obtained using these formalisms compare well with previous data. Hence, these results would be quite useful to the atomic and molecular physics community.

Acknowledgements

Authors would like to acknowledge W. J. Brigg, Department of Physics and Astronomy, University College London, UK for helpful discussions at the early stage of the calculations. BA is pleased to acknowledge the support of this research by the Department of Science and Technology (DST), New Delhi through Grant No. SR/S2/LOP-11/2013.

Notes and references

Department of Applied Physics, Indian School of Mines, Dhanbad,

826004, Jharkhand, India. Tel: +91 9470194795; E-mail:

bka.ism@gmail.com

1. G. G. Devyatikh, E. M. Dianov, N. S. Karpychev, S. M. Mazavin, V. M. Mashinskiĭ, V. B. Neustruev, A. V. Nikolaichik, A. M. Prokhorov, A. I. Ritus, N. I. Sokolov, and A. S. Yushin, *Sov. J. Quantum Electron.* 1980, **10**, 900.
2. L. Wang and J. Zhang, *J. Phys. Chem. A*, 2004, **108**, 10353.
3. K. Sakata and A. Tachibana, *Chem. Phys. Lett.*, 2000, **320**, 527.
4. M. Yamamoto, J. Hanna, and M. Miyauchi, *Appl. Phys. Lett.* 1993, **63**, 2508.
5. C. Szymkowski, P. Mozejko, and G. Kasperski, *J. Phys. B: At. Mol. Opt. Phys.*, 1998, **3**, 3917.
6. H. Kato, A. Suga, M. Hoshino, F. Blanco, G. García, P. Limão-Vieira, M. J. Brunger, and H. Tanaka, *J. Chem. Phys.*, 2012, **136**, 134313.
7. P. Mozejko, B. Żywicka-Mozejko, and C. Szymkowski, *Nucl. Instrum. Methods Phys. Res. Sect. B*, 2002, **196**, 245.
8. J. M. Carr, P. G. Galiatsatos, J. D. Gorfinkiel, A. G. Harvey, M. A. Lysaght, D. Madden, Z. Mašín, M. Plummer, J. Tennyson, and H.N. Varambhia, *Euro. J. Phys. D*, 2012, **66**, 58.
9. J. Tennyson, D. B. Brown, J. M. Munro, I. Rozum, H. N. Varambhia, and N. Vinci, *J. Phys. Conf. Ser.*, 2007, **86**, 012001.
10. D. Gupta, R. Naghma, B. Goswami and B. Antony, *RSC Adv.*, 2014, **4**, 9197.
11. B. Goswami, R. Naghma, and B. Antony, *Phys. Rev. A*, 2013, **88**, 032707.
12. M. Vinodkumar, A. Barot, and B. Antony, *J. Chem. Phys.*, 2012, **136**, 184308.
13. B. Goswami and B. Antony, *RSC Adv.*, 2014, **4**, 30953.
14. See <http://www.wiredchemist.com/chemistry/data/bond-energies-lengths>; for tabulated values of the relevant bond length of the molecule.

15. J. Tennyson, *Phys. Rep.* 2010, **491**, 29.
16. CCCBDB at <http://cccbdb.nist.gov>.
17. K. Takatsuka and V. McKoy, *Phys. Rev. A*, 1981, **24**, 2473.
18. B. I. Schneider and T. N. Rescigno, *Phys. Rev. A*, 1988, **37**, 3749.
19. A. M. Arthurs and A. Dalgarno, *Proc. Phys. Soc. London, Sect. A*, 1960, **256**, 540.
20. A. Faure, J. D. Gorfinkiel, L. A. Morgan, and J. Tennyson, *Comput. Phys. Commun.*, 2002, **144**, 224.
21. M. Gailitis, *J. Phys. B*, 1976, **9**, 843.
22. J. Tennyson and C. J. Noble, *Comput. Phys. Commun.*, 1984 **33**, 421.
23. G. Breit and E. Wigner, *Phys. Rev.*, 1936 **49**, 519.
24. N. Sanna and F. A. Gianturco, *Comput. Phys. Commun.*, 1998, **114**, 142.
25. H. L. Cox and R. A. Bonham, *J. Chem. Phys.*, 1967, **47**, 2599.
26. S. Hara, *J. Phys. Soc. Japan*, 1967 **22**, 710.
27. X. Zhang, J. Sun, and Y. Liu, *J. Phys. B*, 1992, **25**, 1893.
28. G. Staszewska, D. W. Schwenke, and D. G. Truhlar, *Phys. Rev. A*, 1984, **29**, 307.
29. C. J. Joachain, 1983, “*Quantum Collision Theory*” (Amsterdam: North-Holland).
30. E. H. Bjarnason, F. H. Ómarsson, M. Hoshino, H. Tanaka, M.J. Brunger, P. Limão-Vieira, and O. Ingólfsson, *Int. J. Mass spectrom.*, 2013, **339/340**, 45.